도시계획학 석사학위논문

Spatiotemporal Analysis of Drought Vulnerability in Mongolia over Three Decades

몽골지역의 30년 기후자료 분석에 의한

가뭄 취약성 연구

2015년 2월

서울대학교 환경대학원

환경계획학과 환경관리전공

이 지 선

Spatiotemporal Analysis of Drought Vulnerability in Mongolia over Three Decades

지도교수 이 도 원

이 논문을 도시계획학 석사 학위논문으로 제출함
2014년 10월

서울대학교 환경대학원
환경계획학과 환경관리전공
이 지 선

이지선의 도시계획학 석사 학위논문을 인준함
2014년 12월

위 원 장 이 동 수 (**Dong-soo Lee**) (인)

부위원장 박 수 진 (**SooJin Park**) (인)

위 원 이 도 원 (**Dowon Lee**) (인)

Abstract

Spatiotemporal Analysis of Drought Vulnerability in Mongolia over Three Decades

Advised by

Prof. Dowon Lee

February, 2015

submitted by

Jisun Lee

Department of Environmental Planning

Graduate School of Environmental Studies

Seoul National University

Studies of arid and semi-arid ecosystems are meaningful in relation to climate change as drylands are especially vulnerable to desertification and land degradation caused by climatic factors and human activities. Precipitation is often the limiting factor for vegetation productivity in such regions, as they experience low annual rainfall, often less than 500 mm. Numerous studies used the Rain Use Efficiency (RUE), an index derived from vegetation productivity and annual precipitation, as a potential indicator for assessing large scale degradation and for evaluating responses of ecosystems to climate change. This study adopted Soil Moisture Use Efficiency based Drought Stress Index and Drought Vulnerability Index by Do and Kang (2014) and modified it for RUE to assess drought stress and drought vulnerability (i.e. sensitivity) in Mongolia.

The objective of this study was to analyze first, the temporal patterns of RUE and drought vulnerability in respective weather station regions over 27 year period, 1982-2008, in Mongolia by utilizing satellite derived vegetation index, namely NDVI (Normalized Difference Vegetation Index) from the Advanced Very High Resolution Radiometer (AVHRR), of growing seasons (June - September) and 63 local weather stations' precipitation data. Secondly, the spatial pattern of RUE and drought vulnerability was analyzed by mapping with pixel based NDVI and Tropical Rainfall Measuring Mission (TRMM) precipitation data during 1998 to 2008, 11 year period. Lastly, climatic, geological, and land use factors attributing to drought stress were identified through multiple regression analysis.

Analysis of variance (ANOVA) was conducted among four steppe zones represented in 63 local weather stations, and the result showed desert having the

most drought stress and drought vulnerability while steppe had the least drought stress but forest steppe had the least drought vulnerability. Notable regions with high drought stress were found in pixel based map; Bayan Ondor and Shinejinst soums in southern part of Bayankhongor aimag and southern part of Erden soum of Gobi-Altai aimag. Most drought vulnerable soums were Altai, Cogt, and Erdene soums in the most southern part of Gobi-Altai aimag. Regression analysis conducted with aggregated values within each soum illustrated that higher population density, temperature, and RUE indicate higher drought stress condition while higher livestock density and precipitation range lowers drought stress, and drought stress is less experienced in land cover of desert steppe and steppe regions compared to desert.

Utilization of RUE index allowed vegetation productivity forecast, land degradation assessment, and drought response projection in Mongolia. While the satellite derived data sets were useful in long term and regional analyses in Mongolia over three decades, for more accurate assessment and verification of results, comparison to higher resolution data and field survey must be accompanied. In response to changing rainfall patterns and temperature rise, assessment of dryland vegetation productivity and drought vulnerability will be relevant to planning future land management.

Key words: drought vulnerability, rain use efficiency, Mongolia, AVHRR NDVI, climate change
Student Number: 2012-23806

Table of Contents

<Tables>

<Figures>

1. Introduction

Studies of arid and semi-arid ecosystems are meaningful in relation to climate change. In Poulter's recent study on global terrestrial carbon cycle over the past 30 years, it was found that semi-arid biomes have become an "important driver of global carbon cycle inter-annual variability" compared with tropical rainforests (2014). Drylands in particular are vulnerable to desertification, a form of land degradation appear in areas with low precipitation caused by climatic variations and human activities (UN, 1994). In response to changing rainfall patterns and temperature rise, assessment of dryland vegetation productivity and drought vulnerability will be relevant to planning future land management.

Water availability is an important factor in all ecosystems for vegetation productivity, especially in arid and semi-arid lands because they experience low amount of mean annual precipitation by definition – arid land from 60-250mm and semi-arid land from 150-500 mm (Noy-Meir, 1973). Precipitation is recognized as the primary resource that controls terrestrial biological activity in arid and semi-arid environments although not the only one (Rosenzweig, 1968). Sufficient field based studies conducted in arid climates have shown high correlation and determination coefficients ($r = 0.71 \sim 0.97$; $R^2 = 0.52 \sim 0.88$) between net primary productivity and annual precipitation from either linear or curvilinear regressions (Le Houerou 1984; Nicholson and Farrar, 1994; Grist and Mpolokang, 1997; Du Plessis, 1999; Fang et al., 2001; Bai et al., 2008; Narangarav, 2011). Chapin et al. (2011) confirmed that the positive linear relationship between vegetation growth and precipitation starts to decrease at about total annual precipitation of 2,200 mm

per year.

The concept of Water Use Efficiency (WUE) was developed with a concern for plant water availability in crop cultivation and a hope to improve crop production (Sinclair et al., 1984). Sinclair et al. (1984) defined WUE as the ratio of biomass accumulation to plant transpiration or evapotranspiration. While the numerator Net Primary Productivity (NPP) is relatively easier to measure, the denominator plant transpiration or evapotranspiration is difficult to measure, especially in a regional scale. In place of WUE, the Rain Use Efficiency (RUE), the ratio of "annual primary production [to] annual rainfall (i.e. the number of kilograms aerial dry matter phytomass produced over 1 ha in 1 year per millimeter of total rain fallen)," have been used extensively as an indicator of ecosystem productivity in various climatic zones with an advantage of accessibility of NPP and rainfall data (Le Houerou, 1984; Turner, 2004). According to Le Houerou (1984), all other conditions controlled, actual field based RUE figures throughout the arid zones globally tend to fall within "less than 0.5 [kg DM/1ha/1 year/mm] in depleted subdesertic ecosystems to over 10.0 [kg DM/1ha/1 year/mm] in highly productive and well managed steppes, prairies, or savannas" and usually 3.0-6.0 [kg DM/1ha/1 year/mm] in well managed grazing lands.

RUE also has been used as a potential indicator for regional degradation or desertification as remote sensing techniques allow quantitative measurement for estimating primary productivity or precipitation (Prince et al., 1998; Nicholson et al., 1998; Huxman et al., 2004; Veron et al., 2006, Bai et al., 2008). Others have considered RUE as an indicator for evaluating responses of ecosystems to altered precipitation or climate change (Yang et al., 2010; Zhongmin et al., 2010). In these contexts, investigating

temporal and spatial variations of RUE for a region is a meaningful step.

Do and Kang (2014), using their developed proxy index of WUE, Soil Moisture Use Efficiency (SMUE; ratio between productivity index NDVI and soil moisture), assessed drought vulnerability. They claimed that "the relative increase of SMUE to the baseline SMUE" is an indicator of vegetation drought stress expressed as Drought Stress Index (DSI) (Do & Kang, 2014). With DSI, they created Drought Vulnerability Index (DVI) to quantify drought sensitivity relative to drought stress and find sensitive regions undergoing a change of dryness during the study period (Do & Kang, 2014). They used satellite data for both productivity and soil moisture with spatial resolution of 0.25º to calculate SMUE, DSI, and DVI over Northeast Asia dry regions. This study will adopt the concept of DSI and DVI using other proxy index for WUE, namely RUE, to assess drought vulnerability temporally and spatially. The produced result can be used for comparison since they both are WUE based drought vulnerability analysis over the same region.

It is worth noting that for some biomes their precipitation only comes from the rainfall, while others with winter seasons, snow and hail is included in the amount of precipitation. The term RUE has developed from studies mostly done in warm climates where only rainfall represents precipitation. For this study, while Mongolia receives rain as well as snow and hail and should it be fitting to use 'Precipitation Use Efficiency', the widely used and known term Rain Use Efficiency will be used since only summer rains are included in the analysis.

The objective of this study is to analyze first, the temporal patterns of RUE

and drought vulnerability in respective weather station regions over 27 year period, 1982-2008, in Mongolia by utilizing satellite derived vegetation index, namely NDVI, of growing seasons (June - September) and 63 local weather stations' annual precipitation data and secondly, the spatial pattern of RUE and drought vulnerability by mapping with pixel based GIMMS NDVI and Tropical Rainfall Measuring Mission (TRMM) precipitation data during 1998 to 2008. Lastly, climatic, geological, and land use factors attributing to drought stress were identified through multiple regression analysis at the soum level.

With temporal and spatial analysis, this study seeks to answer the following questions: 1) what is the overall range and pattern of RUE in Mongolia?; 2) do natural zones differ in RUE and drought vulnerability?; 3) where are the hot spots or regions that show vegetation vulnerability or sensitivity to changing precipitation?; and 4) what factors attribute to drought stress and vulnerability?

2. Materials and Methods

2.1. Site Description

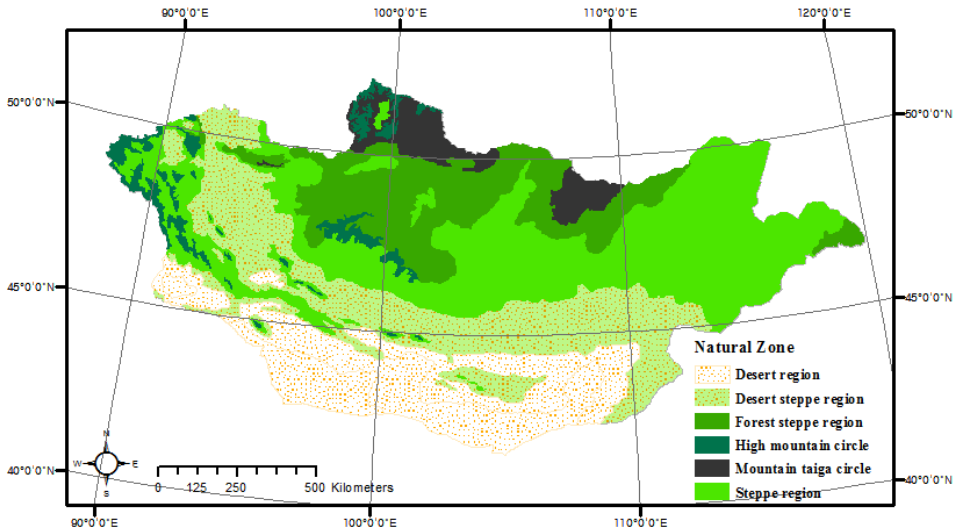

Fig. 1. Natural Zone map of Mongolia, 2005 (Institute of Geoecology, Mongolian Academy of Sciences)

The study site includes the entire territory of Mongolia. Mongolia is located at the latitudes of 41º35'- 52º09'N and longitudes of 87º44' - 119º56'E with area of 1,564 square kilometers (Narangarav & Lin, 2011). Most of its land (Fig.1) is covered with steppe (80%), and some forest (7%) in the north and desert in the south are found (Suttie et al., 2005).

Due to its geographic location in the central Eurasian continent, landlocked and surrounded by high mountains on average 1500 meters, it has a harsh continental climate (Natsagdorj L. and Sarantuya G., 2014). It has short, dry summers, and long, cold winters with fluctuating spring and autumn year to year within a broad range (Fig.3; Natsagdorj L. and Sarantuya G., 2014). 85 % of the total annual precipitation comes during the warm season months, from April to

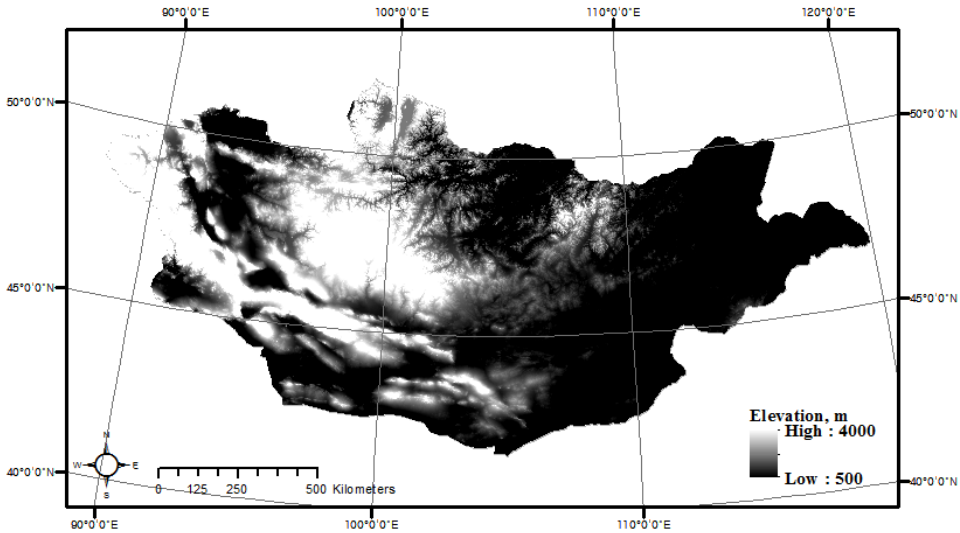

Fig. 2. Elevation map of Mongolia (NASA Shuttle Radar Topographic Mission, approx. 90m resolution; Jarvis et al., 2008)

September, and 50 - 60 % of this precipitation fall in July and August alone (Fig. 4; Natsagdorj L. and Sarantuya G., 2014). The number of rainy days also vary regionally affected by different elevation and land cover (fig. 1 & 2), from 60-70 days in the northern mountainous regions to about 30 days in the south Gobi (Natsagdorj L. and Sarantuya G., 2014). Overall, Mongolia has low amount of precipitation, but with high intensity – any region can experience 50 mm in one day (Natsagdorj L. and Sarantuya G., 2014).

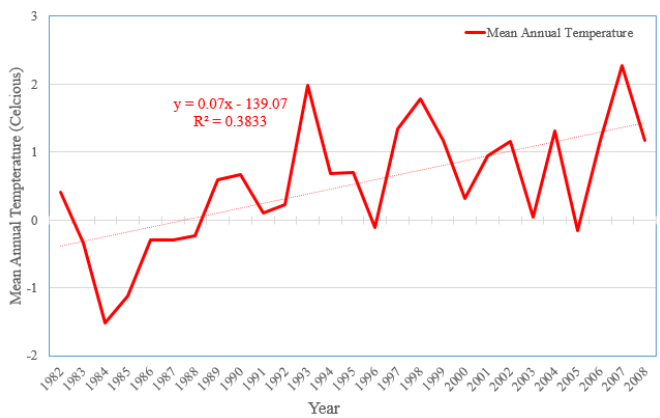

Fig. 3. Temperature change in 63 weather stations over 27 years in Mongolia

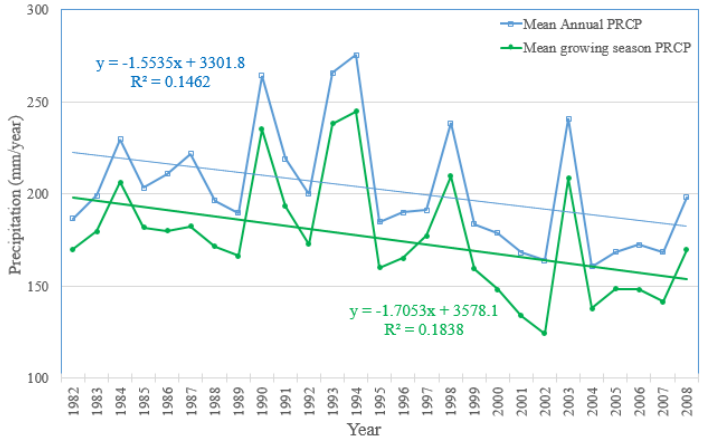

Fig. 4. Precipitation change in 63 weather stations over 27 years in Mongolia (PRCP= Precipitation)

2.2. Data Description

2.2.1. NOAA GIMMS NDVI data set, 1982-2008 (27 years)

For calculation of RUE, normally aboveground net primary productivity (ANPP) is used from collected field data, however, with the long time span of the study period being 27 years and the study region being the entire territory of Mongolia, it is impossible to get accurate ANPP data. The introduction of satellite remote sensing techniques in early 1980s has provided the opportunity to detect and estimate vegetation productivity on a regional scale by Normalized Difference Vegetation Index (NDVI) values derived from satellite images (Prince et al., 1998). NDVI, a satellite derived vegetation index useful for a long time scale and at a vast spatial scale has been the most widely used vegetation index in numerous vegetation and drought monitoring studies (Hellden et al., 2008). Farrar et al. (1994) has claimed that NDVI well correlates with parameters such as leaf area index, green leaf biomass, and vegetation cover. NDVI has been used to estimate aboveground Net Primary Productivity (Ricotta et al, 1999; Paruelo et al., 2014).

NDVI data sets created by the Global Inventory Modelling and Mapping Studies (GIMMS) in particular are values of the difference in reflectance between the Advanced Very High Resolution Radiometer (AVHRR) near-infrared and visible bands divided by the sum of these two bands (Tucker 1980). As the green leaves have a higher reflectance in the AVHRR near infrared band, or band 2, compared to the visible band, or band 1, stronger chlorophyll absorption occurs in the red region, band 1 (Tucker et al., 2010). The difference in vegetation reflectance increases with green leaf vegetation density, or chlorophyll concentration, and this index ranges between -1 and +1 (Tucker et al., 2010).

Therefore, this study relies on the satellite derived vegetation index, namely NDVI provided from the Global Land Cover Facility (GLCF). This GIMMS AVHRR NDVI data sets are satellite imagery records of bimonthly changes in terrestrial vegetation from America's National Oceanic and Atmospheric Administration (NOAA) satellite series, NOAA 7, 9, 11, 14, 16 and 17 since July, 1981 to present day (Fig. 5; Tucker et al., 2010).

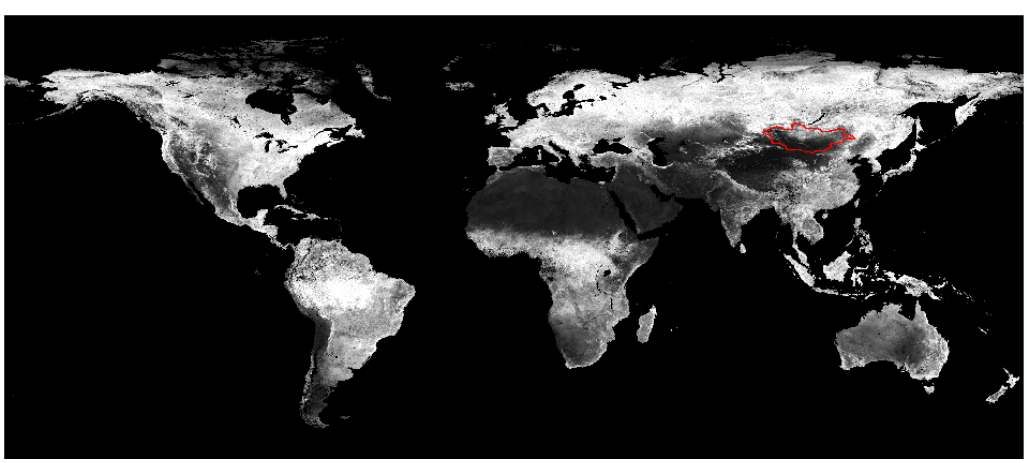

Fig. 5. An example of raw global GIMMS NDVI bimonthly data. Maximum Value Composite imagery of first 15 days in July, 1982. (Data source: GLCF)

The acquired 8-km satellite imageries are processed with radiometric calibration, aerosol correction and cloud screening, satellite drift corrections, and inter-calibration of NDVI with MODerate resolution Image Spectroradiometer (MODIS) and Satellite Pour l'Observation de la Terre (SPOT)-Vegetation data to minimize the variation (Tucker et al., 2010). Its accuracy have been evaluated by Fensholt et al., 2009 and Beck et al., 2011 and the data has been utilized by several studies (Tucker et al., 2003; De Beurs and Henebry, 2008; Alcaraz-Segura et al., 2010). As Terra MODIS NDVI was made available since year 2000 with higher resolution of 1-km and SPOT VGT data with less than 20 m, studies were conducted to evaluate the accuracy of GIMMS NDVI for the overlapping period of available data (Fensholt et al., 2009).

2.2.2. 63 Local Weather Stations Monthly Precipitation data, 1982-2008 (27 years)

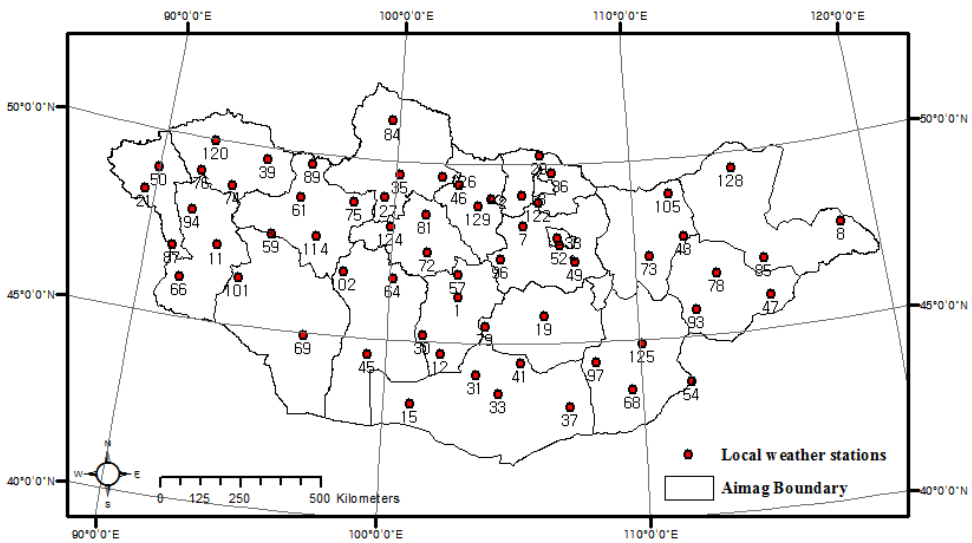

Fig. 6. 63 local weather stations with locations and numbers indicated in the map of Mongolia.

Today, 135 meteorological stations are operating in Mongolia to locally and regularly collect precipitation and other climate data (Natsagdorj L. and Sarantuya G., 2014). However, for the purpose of this study, only those weather stations which have monthly precipitation data since 1982 at hand will be considered. Out of 70 weather stations in the original list, the author checked the completeness of data set, and only 63 stations had monthly precipitation data in the respective location. Thus, 63 local weather stations (Fig.6 & Appendix 1) located throughout Mongolia were carefully selected for this study. The Institute of Meteorology and Hydrology in Mongolia is the source of this data set.

While electronic data collection method has been implemented in the main weather stations recently, at most weather stations, data clerk manually collects and measures precipitation from a pluviometer every three hours for reporting (Fig. 7).

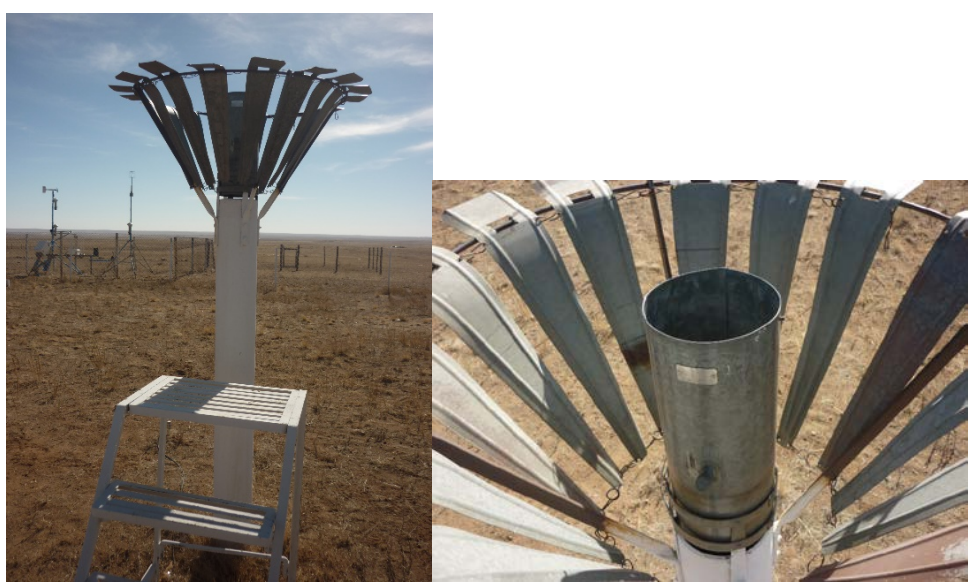

Fig. 7. A pluviometer, an old styled precipitation collecting equipment at one of the local weather stations, Dalanzagad, Omnogobi (#33).

2.2.3. Tropical Rainfall Measuring Mission (TRMM) 3b43, 1998-2008 (11 years)

While point data from 63 local weather stations provide 27-year long data set, they are insufficient to draw a map which can accurately represent the precipitation distribution of Mongolia. To serve the purpose of spatial analysis of precipitation and RUE through mapping, satellite derived and pixel based precipitation data of Tropical Rainfall Measuring Mission (TRMM) was also used in this study (Fig 8). The TRMM data is also with GIMMS NDVI, another pixel based data set. The TRMM data set is available since 1998, and thus only for the last 11 years of the study period, RUE maps will be produced.

TRMM 3b43 data set is produced by a joint mission between NASA and Japan Aerospace Exploration Agency. This set of global precipitation data is available at 25 km spatial resolution and monthly temporal resolution. While its name, “Tropical Rainfall” Measuring mission, has a connotation that the data set was intended only for tropical biomes, the global data has been used widely for all biomes. TRMM has been used for global semi-arid land studies such as Tunisia, Senegal, Saudi Arabia, and Namibia, and studies show that it can be applied for grassland shrubland, while bare and desert areas may give false alarms (Wang et al., 2009; Almazroui, 2011; Hüttich et al., 2011; Tarnavsky et al., 2012; Tarnavsky et al., 2013; Poulter et al., 2014).

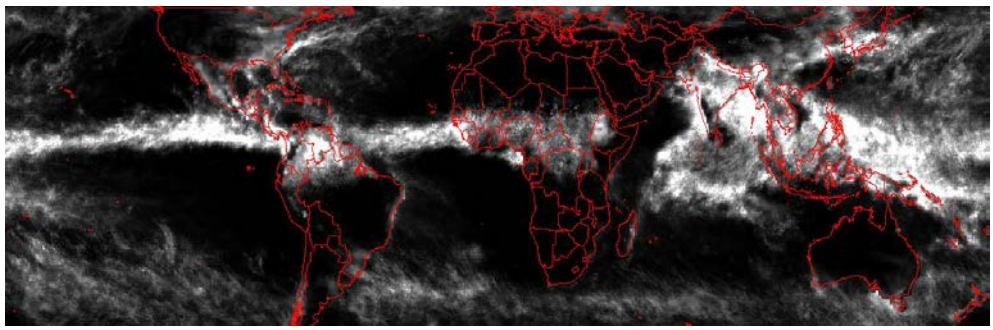

Fig. 8. An example of a rotated (270 degree) raw TRMM data for the month of July, 2003. (The world map in red purposely drawn to indicate the location of Mongolia.)

2.3 Data Analysis

2.3.1. Weather Station based RUE and Drought Vulnerability (27 years)

Upon preparing bimonthly GIMMS NDVI data for growing season of June, July, August and September during the 27 year study period, 1982-2008 (8 images per year), projected coordinate system was set to World Geodetic System (WGS) 1984, Universal Transverse Mercator(UTM) zone 48 North with Transverse Mercator as projection using ENVI version 5.1 software program. Then, Mongolia was extracted by its national boundary from the global map. 8 images for each year were accumulated and made into one map. For total of 27 years, 27 growing season maps were created via ENVI version 5.1.

On ArcGIS version 10.1, using “extract values to points” in Spatial Analyst Tools, NDVI values were extracted from the pixels 63 weather stations points were laying. This was done for all 27 years to create NDVI values corresponding to growing season precipitation data for 63 weather stations.

From the monthly precipitation data set for 63 weather stations, four growing

season months data were combined for each year of 1982-2008.

Prepared growing season NDVI for each year were divided by growing season precipitation data from all 63 weather station points in Microsoft Excel to produce weather station based RUE (Eq.1). For statistical analysis, analysis of variance was conducted among four natural zones, desert, desert steppe, forest steppe, and steppe using Pairwise Wilcoxon Rank Sum Tests in R package program.

$$\textbf{Rain Use Efficiency} = \frac{\text{summed NDVI of growing season}}{\text{summed precipitation of growing season}} \qquad \textbf{(Eq.1)}$$

For drought vulnerability assessment was conducted based on methods done in Do and Kang (2014). As in Do and Kang (2014), in order to use the relative increase of RUE from the baseline to explain vegetation drought stress, RUEbase was first calculated from three wettest years among 27 years based on the growing season precipitation average. The corresponding three RUEs were then taken to be averaged, and RUEbase was calculated in R. For each 27 year, Drought Stress Index (DSI) were produced by following the equation below (Eq.2).

$$\textbf{Drought Stress Index} = \frac{(\text{RUE} - \text{RUEbase})}{\text{RUEbase}} \qquad (\textbf{Eq}.\ 2)$$

Another index to measure drought vulnerability was developed in Do and Kang (2014) using Soil Moisture Use Efficiency. With summed precipitation of growing seasons, Drought Vulnerability Index (DVI) can be made to measure the sensitivity of vegetation productivity to change in precipitation in the case of this study (Eq 3). The negative slope of best fit regression model between previously obtained DSI and summed growing season precipitation will be the DVI, and β will

be the interception coefficient of the regression in this study.

DSI = (- **Drought Vulnerability Index**) * Precipitation for growing season + β

(**Eq**. 3)

As assumed in Do and Kang's study with SMUE, highly vulnerable regions may be indicated through a significant negative slope, having sensitive response to less water availability – or drought stress (2014). Secondly, degradation during the study period may be indicated through a significant positive slope of DVI (Do & Kang, 2014). Lastly, when a flat slope is found, it will indicate already degraded state or experiencing moderate water stress (Do & Kang, 2014).

Drought Stress Index was first calculated, and box plots were drawn for four zones. Based on Drought stress Index, Drought vulnerability Index was calculated and boxplots were drawn to see whether natural zones have different ranges and values using 27 year data.

2.3.2. Map based RUE and Drought Vulnerability (11 years)

1) TRMM data accuracy evaluation

For the purpose of checking whether TRMM 3b43 precipitation data set can be used for RUE mapping in place of local weather station data, monthly TRMM data for all growing season months for study period were prepared. First, each imagery must be rotated 270 degrees and georeferenced in ENVI. Once projected coordinate system was set to WGS 1984, UTM zone 48N and Transverse Mercator

as its projection, each imagery was saved as a GeoTIFF file.

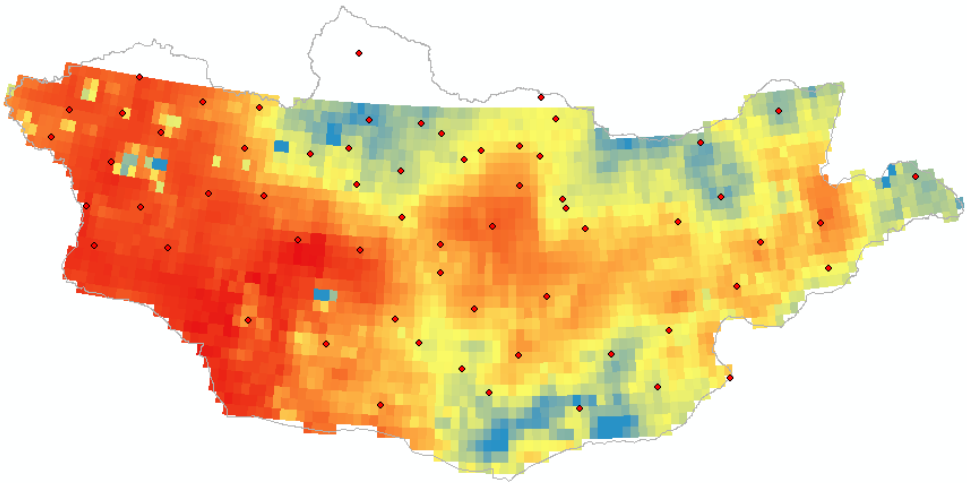

Fig. 9. An example of a monthly TRMM data set and 63 weather station points. Note that two weather stations in the north are not included in the TRMM data.

They were then called in software R Studio version 3.1.2. to be calculated into monthly data form (mm/month) from hourly data form (mm/hr) using sp, raster, and rgdal packages which allow spatial data to be read and written in R. For June and September, TRMM 3b43 * 24 hours * 30 days was calculated and TRMM 3b43 * 24 hours * 31 days for July and August by coding. Only then, calculated monthly data was masked out with the boundary of Mongolia shape file. TRMM data set of Mongolia was now opened in ArcGIS, and using “extract values to points” in Spatial Analyst Tools, TRMM data based precipitation values were extracted from the pixels weather stations points were laying. Because TRMM data does not fully cover the country boundary of Mongolia to the far north, only 61 weather station points were extracted for comparison (Fig. 9). This was done for all four months of 11 years of study period with TRMM data availability, 1998-2008.

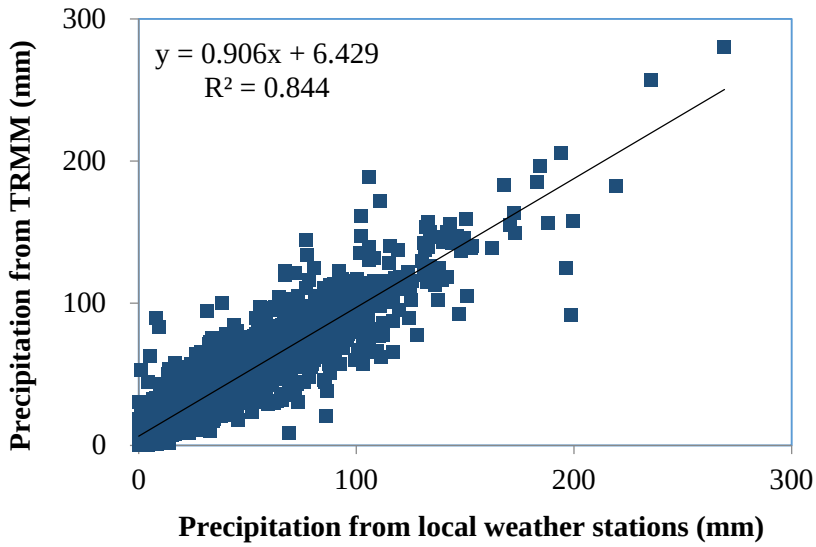

Figure 10. Correlation graph between precipitation data from 61 local weather stations and satellite derived TRMM data set.

Correlation analysis was conducted in Excel between extracted TRMM precipitation values and local weather station precipitation data (Fig. 10). A statistically significant positive correlation was found between TRMM and local weather stations data on 61 points for all TRMM data in the study period with R square of 0.844 and slope value of 0.906. With this exercise, it was concluded that pixel based TRMM data can replace the point local weather station data to draw pixel based RUE maps with pixel based NDVI data for years of 1998-2008 (Lee and Noh, 2012). .

2) RUE mapping

First of all, on ArcGIS growing season pixel based data for months of June, July, August, and September from GIMMS NDVI and TRMM precipitation were combined each for the study period. Map algebra (Raster calculator) in Spatial

Analyst tools was used to divide NDVI raster file by respective TRMM raster file for each year. Eleven RUE maps were created for each year, and they were averaged. In addition, on R Studio, with loaded packages of sp, raster, and rgdal, average NDVI map and average precipitation map were drawn, as well as coefficient of variation maps for NDVI and precipitation to see the variability over 11 years. Correlation coefficient map between NDVI and precipitation was also drawn.

3) Drought Vulnerability mapping

On R Studio, with loaded packages of sp, raster, and rgdal, NDVI, TRMM precipitation, and RUE maps were first made into same resolution and dimension by resampling and then stacked each with eleven maps. As in Do and Kang (2014), in order to use the relative increase of RUE from the baseline to explain vegetation drought stress, RUEbase was first calculated from three wettest years among 11 years based on the growing season precipitation average. The corresponding three RUEs were then taken to be averaged, and RUEbase map was created in R. With the RUEbase map, for each eleven year, Drought Stress Index (DSI) map can be produced by Eq.2.

With summed precipitation of growing seasons, Drought Vulnerability Index (DVI) was calculated based on eq.2. The negative slope of best fit regression model between previously obtained DSI and summed growing season precipitation will be the DVI, and β will be the interception coefficient of the regression in this study. This pixel based map will be useful as it provides the spatial distribution of vulnerable or sensitive regions to negative change in precipitation (i.e. decrease in precipitation) in Mongolia.

As assumed in Do and Kang's study (2014) with SMUE, highly vulnerable regions may be indicated through a significant negative slope, having sensitive response to less water availability – or drought stress. Secondly, degradation during the study period may be indicated through a significant positive slope of DVI. Lastly, when a flat slope is found, it will indicate already degraded state or experiencing moderate water stress.

2.3.3. Multiple Regression Analysis

For the purpose of finding a relationship between Drought Stress Index and climatic, geological, and land use factors and quantifying the degree of their impact, multiple regression analysis was conducted.

DSI was chosen to be the responsive variable y, and annual mean temperature, growing season precipitation, growing season NDVI, RUE, land cover, digital elevation model (DEM), slope, aspect, livestock density, and population density were the initial input explanatory variables x (Table 1). Stepwise selection method was done to reach the final regression model. The variables with low p-value (< 0.05) were only included in the next regression test. Package R was used in the regression analysis.

Out of 333 soums in Mongolia, 268 soums with all available data were included in the analysis as sample. All variables were averaged by soum boundary to give a representative value using zonal statistics in ArcGIS software. Empty or two thirds empty soums at the upper part of Mongolia due

to data missing from TRMM data were excluded for accurate data analysis.

Table 1. Data description for regression analysis.

Data	Available year(s)	Source
Growing season (6-8) mean temperature	2003-2008	Jang et al., 2014
Growing season (6-9) precipitation	1998-2008	Tropical Rainfall Measuring Mission (TRMM)
Growing season (6-9) NDVI	1998-2008	Global Inventory Modeling and Mapping Studies (GIMMS), Global Land Cover Facility
Rain Use Efficiency	1998-2008	This study
Natural zone (Land cover)	2005	Institute of Geoecology, Mongolian Academy of Sciences
Digital Elevation Model (DEM), 90 m	2008	Shuttle Radar Topography Mission (SRTM), Jarvis et al., 2008
Slope	2008	Created in ArcGIS with DEM from Jarvis et al., 2008
Aspect	2008	Created in ArcGIS with DEM from Jarvis et al., 2008
Livestock density	1998-2008	LEWS (Livestock Early Warning System) project in Mongolia
Population density	2003-2008	Mongolia National Statistical Information service
Drought Stress Index	1998-2008	This study

3. Results

3.1. Weather Station based Rain Use Efficiency

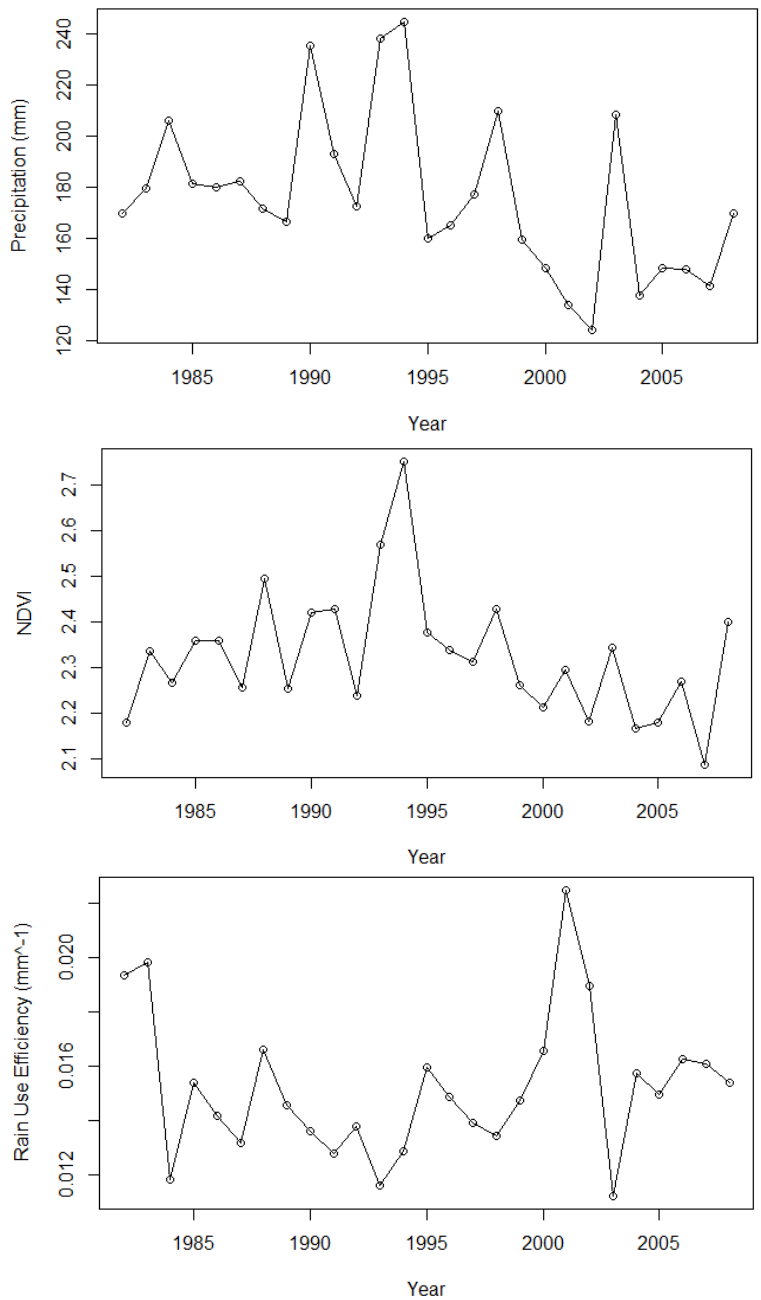

Fig. 11. Mean NDVI, mean Precipitation, and mean RUE changes for all 63 weather station sites during 1982-2008.

Figure 11 illustrates interannual changes of NDVI, precipitation and RUE with all yearly data points of 63 weathers stations over 27 years. Overall, as precipitation increases, NDVI also tends to increase. Precipitation decreased extensively in the year of 2001, 2002, and 2003, but compared to the magnitude of the precipitation dip, NDVI did not rapidly fall as much. Consequently, in the same years, RUE has rapidly shot up having almost unchanged NDVI with a large drop of precipitation.

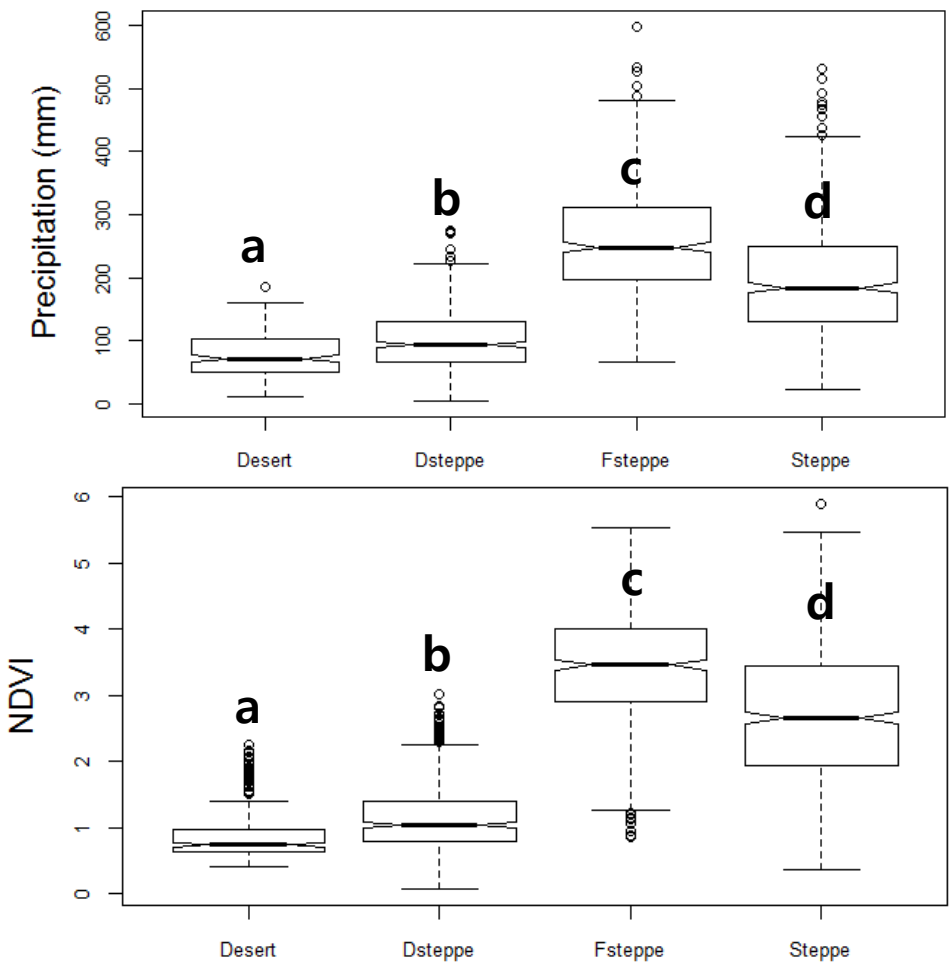

Fig. 12. Precipitation and NDVI boxplots by four zones, Desert, Desert Steppe (Dsteppe), Forest Steppe (Fsteppe), and Steppe.

Analysis of variance (ANOVA) was conducted among four natural zones, desert, desert steppe, forest steppe, and steppe using Pairwise Wilcoxon Rank Sum Tests in R package program. For precipitation and NDVI, all four zones were verified as each clearly belonged to a different group as seen in figure 12. As can be seen from the boxplot of precipitation, the desert zone has the least amount of rainfall of approximately 77 mm during the growing seasons, then, desert steppe, steppe, and forest steppe in order. For summed NDVI during the growing seasons, the mean also differs distinctively as the desert zone has less than 1.0, desert steppe zone with just above 1.0, steppe zone greater than 2.5, and finally the forest steppe zone with just less than 3.5. For both precipitation and NDVI, the variances were found to be relatively small in the desert and desert steppe, and steppe had the biggest variance as shown in table 2. Figure 13 illustrates the distinct NDVI and precipitation ranges among different zones.

Table 2. Mean and standard deviation (sd) of precipitation, NDVI, and Rain Use Efficiency for each zone.

Zone	**Precipitation (mm)**		**NDVI**		**Rain Use Efficiency (mm^{-1})**	
	Mean	*Sd*	*Mean*	*Sd*	*Mean*	*Sd*
Desert	77.731	35.998	0.9205	0.449	0.0171	0.0202
Desert Steppe	102.317	48.776	1.1958	0.559	0.0156	0.0208
Forest Steppe	258.031	82.487	3.4234	0.889	0.0144	0.00534
Steppe	195.435	85.435	2.691	1.1067	0.0150	0.00632

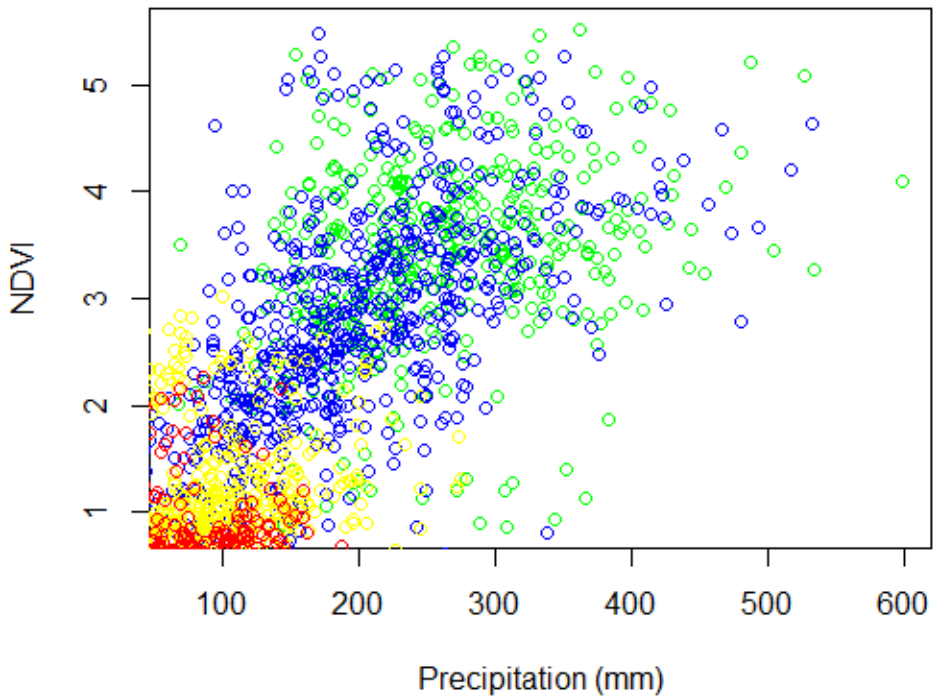

Figure 13. Relationship between growing season NDVI and growing season precipitation.

(Desert: red, Desert steppe: yellow, Steppe: blue, Forest Steppe: green)

In the case of RUE, ANOVA test indicated that desert and desert steppe are in the same group and forest and steppe are in another group together (Fig.14). Desert and desert steppe zones have similar mean values compared to forest steppe and steppe zones (Table 2). Moreover, their standard deviations clearly make them one group, since they are four times bigger than forest steppe and steppes zones'. Interestingly, mean RUE is highest in desert, second highest in desert steppe, third highest in steppe, and lastly forest steppe. With fourfold bigger variance in the desert and desert steppe zones, it appears that these zones are less stable compared to forest steppe and steppe in their vegetation productivity.

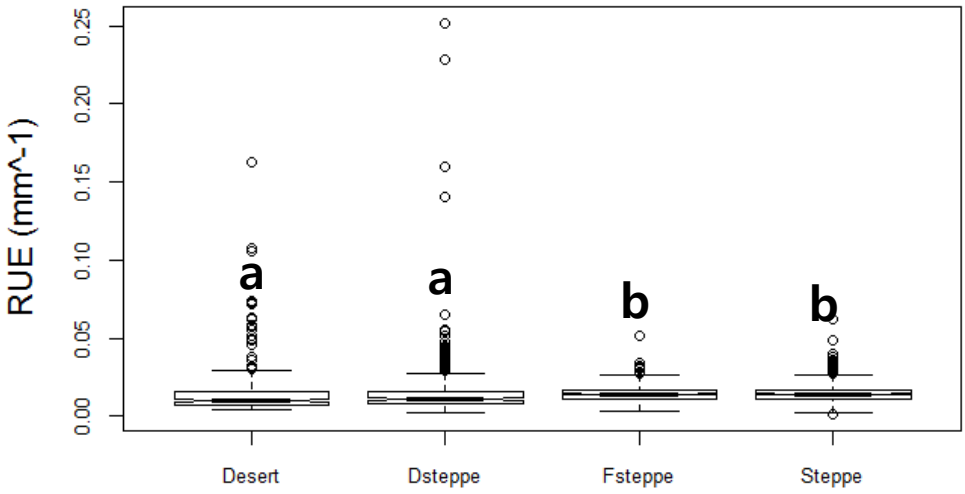

Fig. 14. Rain Use Efficiency boxplot by four zones, Desert, Desert Steppe (Dsteppe), Forest Steppe (Fsteppe), and Steppe.

3.2 Weather Station based Drought Vulnerability

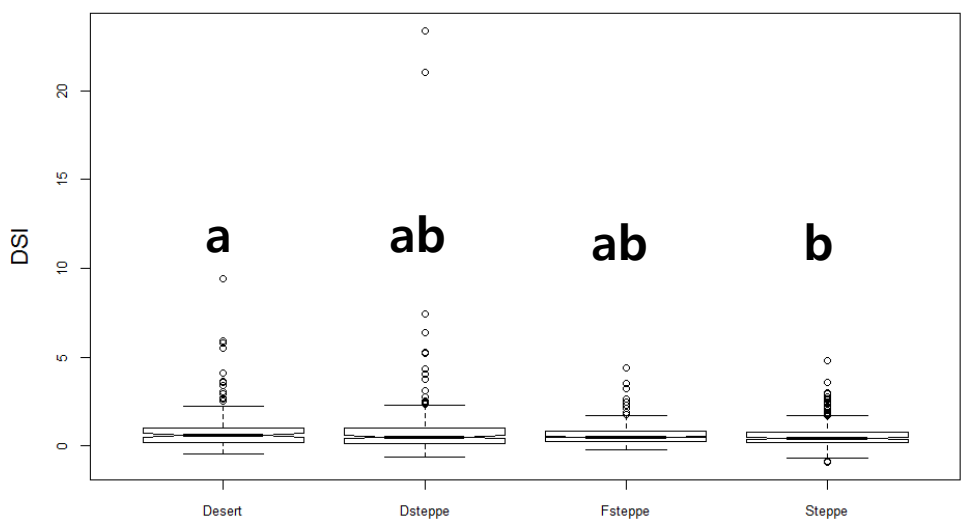

Fig. 15. Boxplot for drought stress index by four zones.

The result of Drought Stress Index, being the relative increase of RUE to the baseline RUE, largely resembles RUE boxplot (Figure 15). However, when

ANOVA tested, while desert and steppe zones are clearly from a different group, desert steppe and forest steppe zones are related to both desert and steppe zones. Desert has the highest mean of DVI, and desert steppe, forest steppe, and steppe in order (Table 3). Desert and desert steppe has larger variance than forest steppe and steppe zones. The steppe zone appears to have the least drought stress.

Table 3. Mean and standard deviation (sd) of Drought Stress Index and Drought Vulnerability Index for each zone.

Zone	**Drought Stress Index**		**Drought Vulnerability Index**	
	Mean	*Sd*	*Mean*	*Sd*
Desert	0.870	1.201	0.0204	0.0148
Desert Steppe	0.814	1.765	0.0175	0.0200
Forest Steppe	0.603	0.555	0.00612	0.00203
Steppe	0.541	0.596	0.00669	0.00380

From the boxplot in figure 16, it is clear that desert and desert steppe suffer much drought vulnerability with their high mean DVI compared to the forest steppe and steppe zones'. ANOVA test indicates that desert and desert steppe belong to a different group, while forest steppe and steppe are from the same group. Mean and standard deviation of forest steppe and steppe are quite similar.

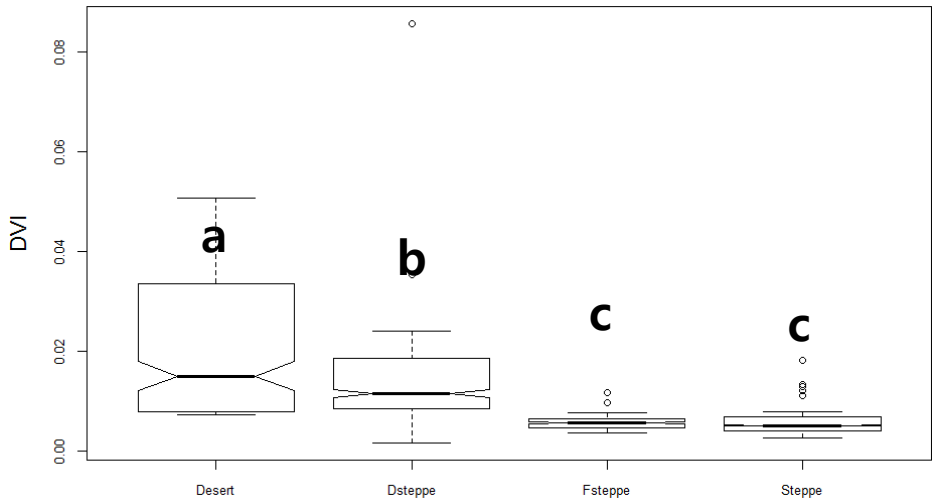

Fig. 16. Boxplot of Drought Vulnerability Index by four zones.

3.3 Map based Rain Use Efficiency

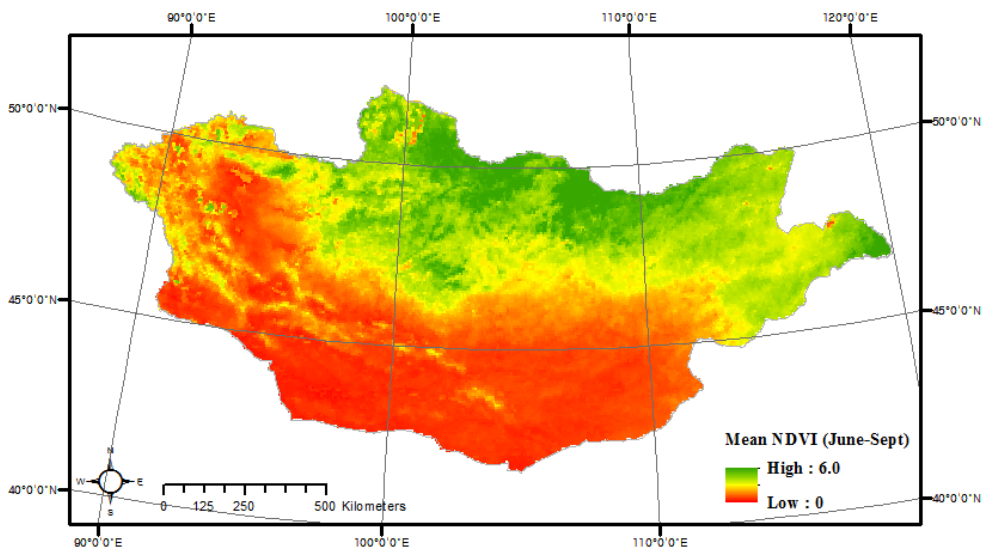

Fig. 17. Mean NDVI of 27 year growing season data.

The mean NDVI of 27 year GIMMS NDVI data for growing season shows clearly varying pattern of vegetation status throughout Mongolia (Fig. 17). In the

northern part of Mongolia where covered by forest shows high NDVI, whereas in the south, in the desert and desert steppe show much low NDVI distribution.

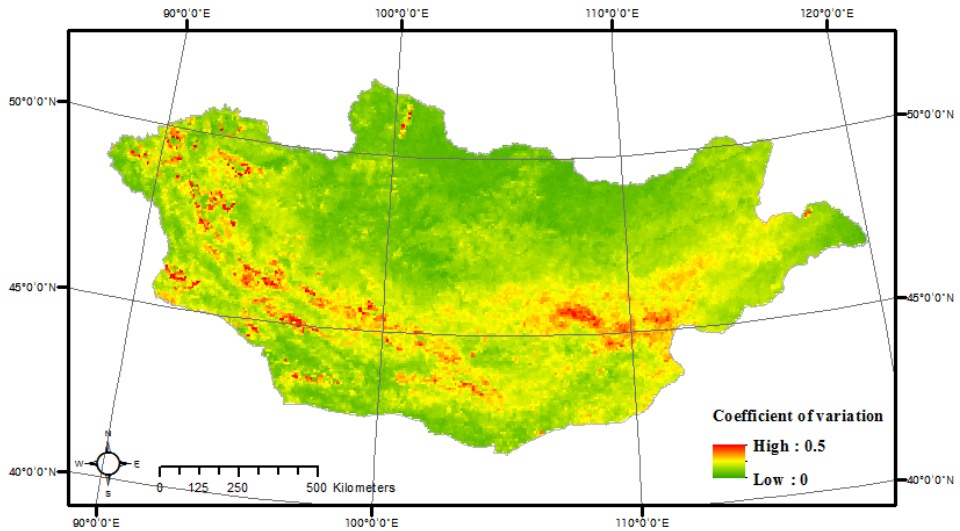

Fig. 18. Coefficient of variation map of growing season NDVI, 1982-2008.

The coefficient of variation of NDVI for 27 years study period was drawn in a map as seen in figure 18. Dornogovi and Dungovi aimags in the east and gobi desert regions show higher between year variations in NDVI. Northern part where mostly covered with high mountains and steppes showed less variability.

Mean Precipitation map produced from TRMM data for 11 year period showed expected spatial pattern of precipitation fallen during the growing season (fig 19). In the northern part, there was more precipitation while much smaller amount of precipitation were fallen in the south. The coefficient of variation map of precipitation shows interesting pattern where apart from mountainous regions in the center of Mongolia with Arkhangai Mountain and far west, variability of precipitation was relatively evenly distributed throughout the rest of the country (fig.20). It shows Mongolia has very high interannual variability of precipitation.

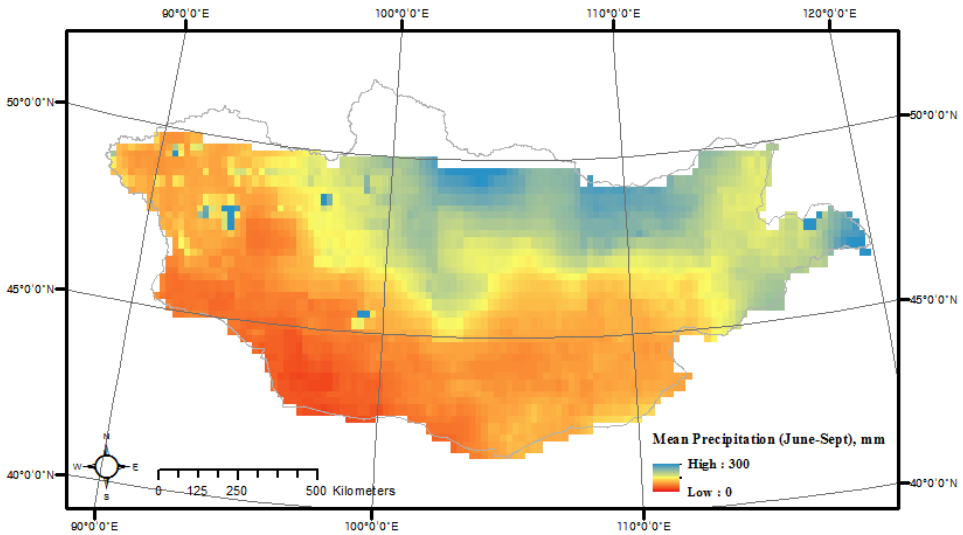

Fig. 19. Mean precipitation map produced from TRMM data for growing seasons of 1998-2008.

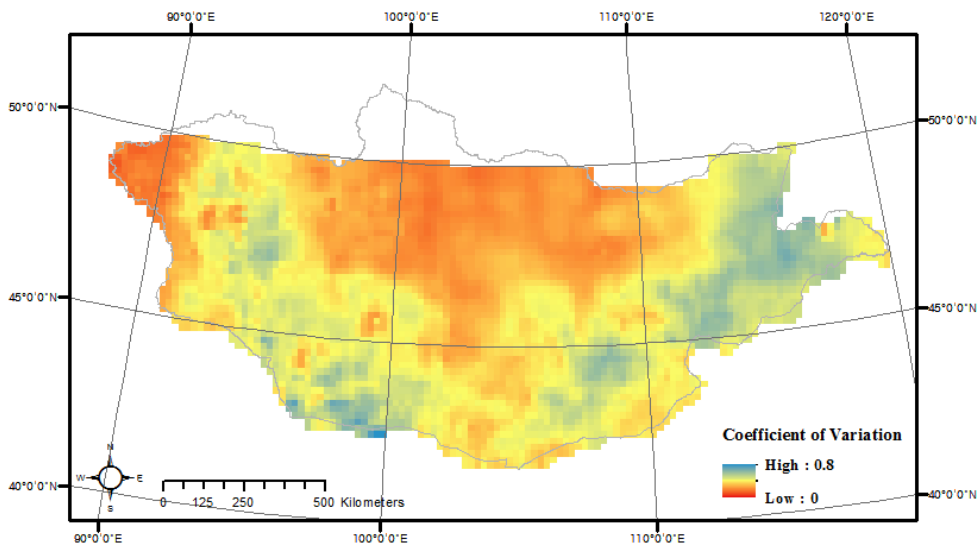

Fig. 20. Coefficient of variation map of growing season precipitation, 1982-2008.

The spatial pattern of correlation between NDVI and precipitation for 11 overlapping years showed flat steppe regions with higher correlation, while on the mountainous area in the northern part and south western part, there was low correlation between NDVI and precipitation (Fig.21). The blue parts are mostly flat

steppe regions.

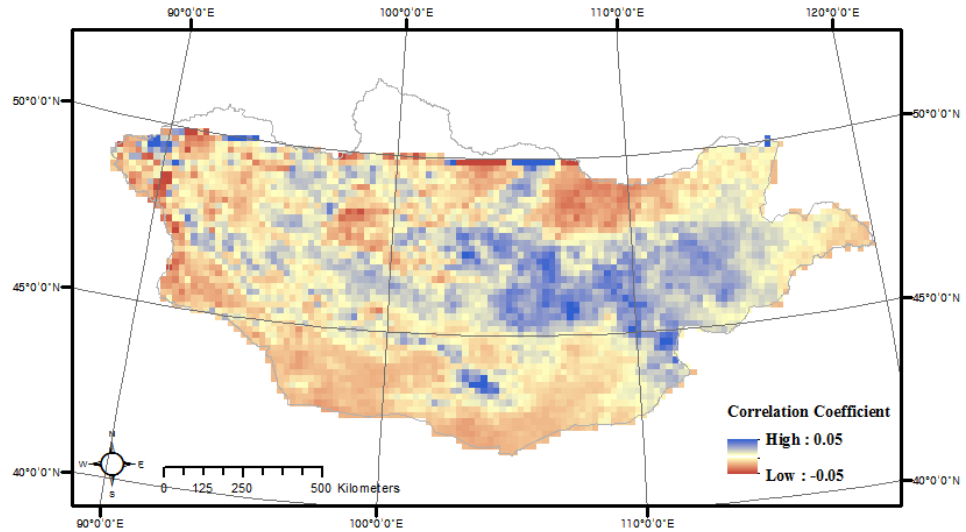

Fig. 21. Correlation coefficient map between NDVI and precipitation for 1998-2008.

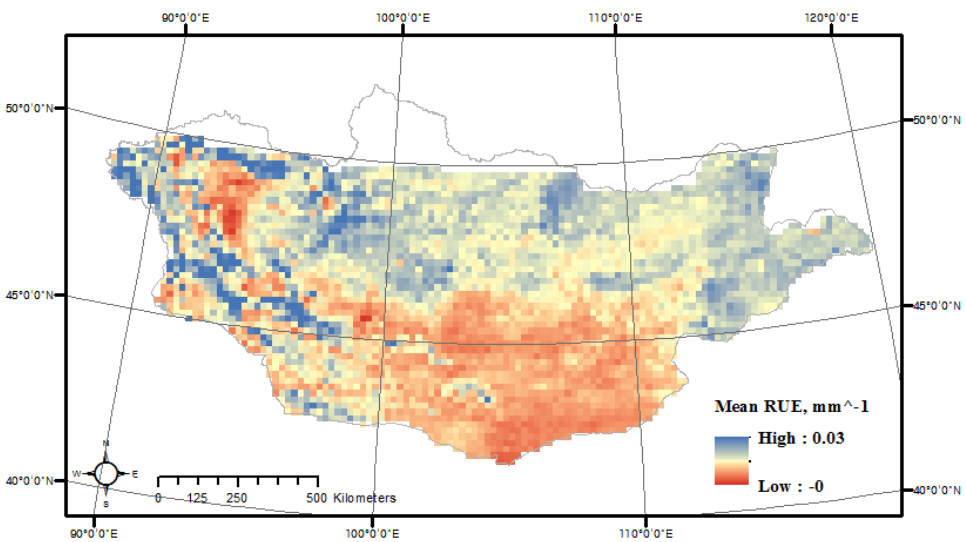

Fig. 22. Mean RUE map of Mongolia, 1998-2008.

RUE map averaged from 11 years were created (Fig. 22). RUE values were lower in the south in general and higher in the northern part where mountain steppes

and steppes are present. RUE base map (Fig. 23) shows similar pattern to the mean RUE map, except the Arkhangai mountain region in the center, where it has higher RUE compared to the mean RUE map. In the eastern part of Mongolia, RUE base has lower values that mean RUE map. In general, RUE base map has lower RUE values than the mean RUE map.

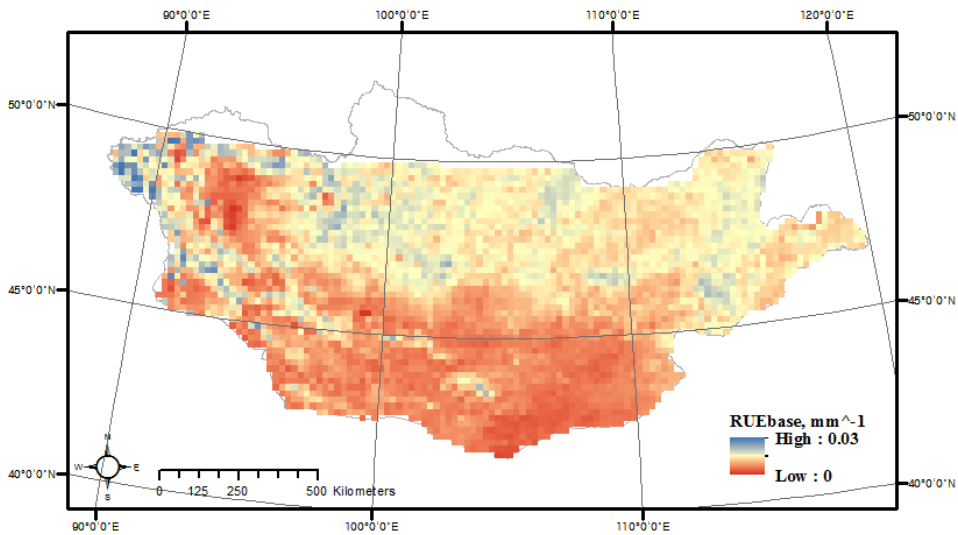

Fig. 23. RUE base map of Mongolia, 1998-2008

3.4 Map based Drought Vulnerability

The mean DSI map showed less stressed conditions of water availability in Mongolia, especially in the central region mostly covered with steppe. Notable regions with high drought stress were found in Bayan Ondor and Shinejinst soums in southern part of Bayankhongor aimag and southern part of Erden soum of Gobi-Altai aimag (Fig. 24 & 26). Most drought vulnerable soums were Altai, Cogt, and Erdene soums in the most southern part of Govi-Altai aimag (Fig. 25 & 26).

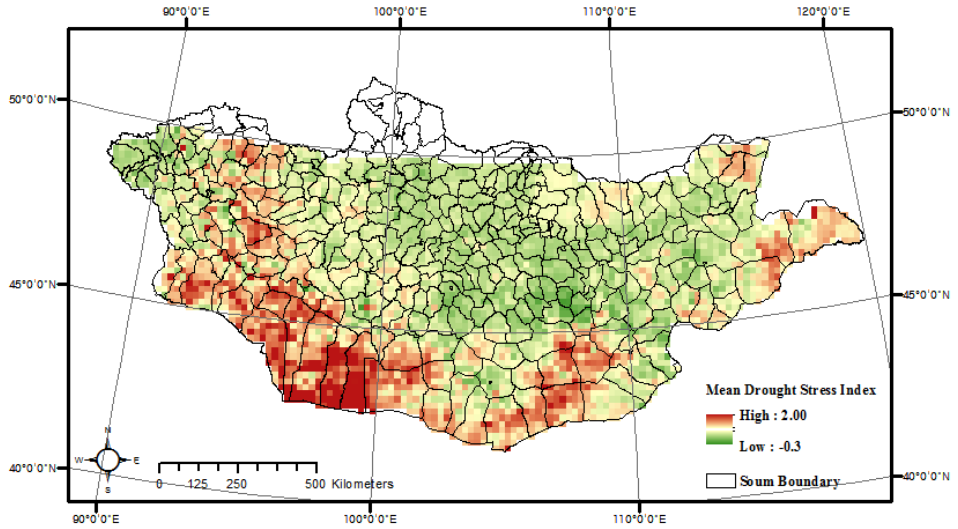

Fig. 24. Mean Drought Stress Index map, 1998-2008

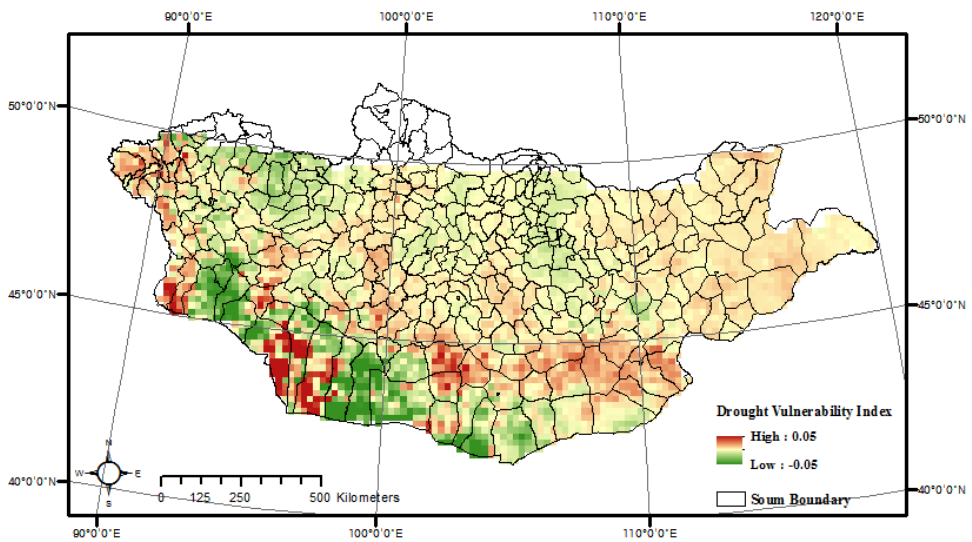

Fig. 25. Drought Vulnerability Index map, 1998-2008

The mean DSI distribution compared to the DVI has some similarities and differences. As seen in the DSI map, five soums in the southwestern part of Mongolia suffers most drought stress, and they are Altai, Cogt, Erdene, Bayan Ondor, and Shinejinst soums. However, among them, Bayan Ondor and Shinejinst soums show negative DVI while other three show positive DVI. The soums with positive DVI

suggest that they are highly vulnerable to drought stress, and the soums with negative DVI indicate that they underwent degradation during the 11 year study period (Do & Kang, 2014). T

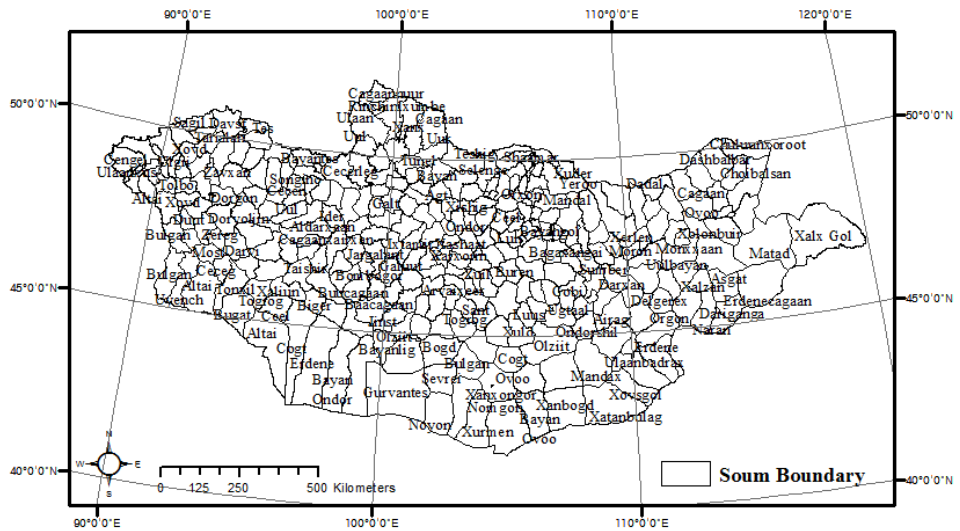

Fig. 26. Soums with labels

3.5. Multiple Regression Analysis by soums

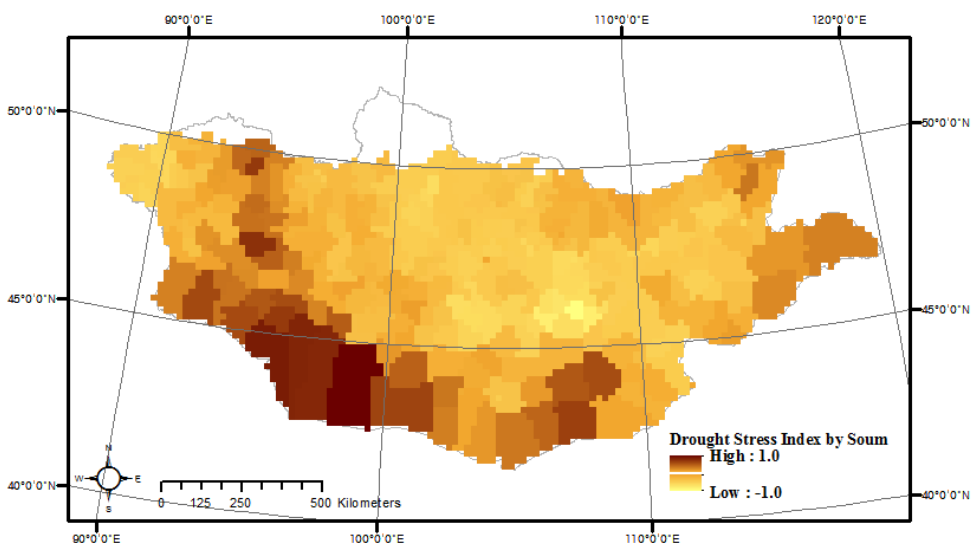

Fig. 27. Averaged Drought Stress Index by soum (y variable).

After testing collinearity for all x and y variables, slope, NDVI, and RUE were excluded because their correlation coefficient with other variables were higher than 0.8 (Lee and Noh, 2012).

With averaged soum level DSI as y variable (Fig. 27), a final regression model was chosen. Regression analysis conducted at the soum level illustrated that higher population density, temperature, and RUE indicate higher drought stress condition while higher livestock density and precipitation range lowers drought stress, and drought stress is less experienced in land cover of desert steppe and steppe regions compared to desert. This model explained 40.26 % (adjusted $r^2 = 0.4026$) of the y variable, DSI.

Table 4. Summary of the final regression model.

X variable	Estimated coefficient	Standard Error	t value	P value	Data type
Livestock density	-0.491	0.0947	-5.183	4.42e-07 ***	Numeric
Population density	1.059	0.261	4.050	6.77e-05 ***	Numeric
Temperature	0.00664	0.00267	2.484	0.01363 *	Numeric
RUE	14.560	2.629	5.537	7.56e-08 ***	Numeric
Precipitation	-0.00134	0.000231	-5.798	1.95e-08 ***	Numeric
Land cover: Desert Steppe	-0.125	0.0504	-2.474	0.01400 *	Factor with 5 levels
Land cover: Forest Steppe	-0.0930	0.0686	-1.356	0.176	Factor with 5 levels
Land cover: Mountain Taiga Circle	-0.110	0.102	-1.080	0.280	Factor with 5 levels
Land cover: Steppe	-0.1649	0.0583	-2.828	0.00504 **	Factor with 5 levels
Intercept	-1.381	0.805	-1.716	0.0874	-

Significant codes: 0 '***', 0.001 '**', 0.01 '*'

The selected final regression model was:

$$y = -0.491(\text{Livestock density}) + 1.059(\text{Population density}) + 0.007(\text{Temperature}) + 14.600(\text{RUE}) - 0.001(\text{Precipitation}) - 0.125(\text{Desert Steppe;factor}) - 0.165(\text{Steppe;factor}) - 1.381$$

4. Discussion

4.1. RUE and DVI among different natural zones

Analysis of variance (ANOVA) among four natural zones, desert, desert steppe, forest steppe, and steppe using Pairwise Wilcoxon Rank Sum Tests in R package program showed clearly four zones have distinctive mean and variance. However, analysis on RUE, showed that forest steppe and steppe are in the same group, while desert and desert steppe are in another group together. Other RUE studies concluded that RUE differ with biomes and vegetation composition (Le Houreou, 1984; Bai et al., 2008; Yang et al., 2010; Zhongmin et al., 2010). With such result from this study, it appears that satellite derived RUE was not able to detect clearly vegetation composition and other environmental factors. In the desert region, NDVI could have been overestimated due to reflecting bare soils and in the forest region, with dense canopy from trees, it could have been underestimated.

Drought Stress Index indicated that desert and desert steppe are under much drought stress, and steppe has the least drought stress. It can be understood as the forest steppe having tall tress to supply water, there is more drought stress than steppe zones, which are covered by vegetation that does not require too much water. In the case of drought vulnerability, three times higher drought stress is experienced in desert compared to the forest steppe and steppe zone which are almost exactly the same in drought vulnerability. Desert steppe also experiences drought vulnerability twice as higher than forest steppe and stepped zones. This implies that for future drought management, it is clear that more effort and

intervention must be done toward desert and desert steppe area.

4.2. Comparison to other Soil moisture derived DSI and DVI

DSI and DVI were first developed and introduced by Do and Kang for the purpose of assessing drought vulnerability of Northeast Asia dryland regions using soil moisture based water use efficiency (2014). Since a part of their study area includes Mongolia, the produced map from this study can be compared with theirs. Although their study period was 25 years, and the map produced from this study only covers 11 years, it is worth comparing two Water Use Efficiency based indices, RUE and SMUE.

DSI and DVI maps from this study do show similar patterns with Do and Kang's map using SMUE. Especially their maps on DSI show similar high drought stress regions in the east and low drought stress region in the central Mongolia. DVI has similar patterns in the south that is where high drought vulnerability regions are southwestern Gobi region.

At the absence of accurate WUE data, both SMUE derived DSI and DVI and RUE derived DSI and DVI are valuable information as to which regions may suffer more under drought stress and less water availability in the future.

4.3. Comparison to published Desertification map

The Center for Desertification Study at the Institute of Geoecology, Mongolian Academy of Sciences regularly publishes a book with numerous maps related to desertification in each decade. Tsogtbaatar et al., 2014 is published for the

purpose of policy making and implementation to reduce the impact of desertification. Their published maps of the soil erosion by wind might explain the notable five soums (Fig. 24 &25) in the southwestern part with high DSI and DVI from this study. From year 2000 to 2010, the soil erosion by wind has largely increased in those soums according to Tsogtbaatar et al., 2014. A map of desertification factors in this book also indicates that in fact those five soums show desertification and the dominant factor is wind erosion (Tsogtbaatar et al., 2014).

5. Conclusions

Utilization of RUE index allowed vegetation productivity forecast, land degradation assessment, and drought response projection in Mongolia. It was shown that different natural zones have their unique range of values of NDVI, PRCP, RUE and DVI, and therefore one set value cannot explain the vegetation productivity of Mongolia. Desert and desert steppe zones have highest drought vulnerability according to 63 weather station data set over 27 years. In mapping, southern Gobi part of Mongolia is suffering drought stress and drought vulnerability. While summer rains may indirectly forecasts the winter rains, since RUE used in this study only includes summer precipitation, the results of this study may not directly forecasts the sensitivity of Mongolian land to the winter precipitation (i.e. snow). Although the satellite derived data sets were useful in long term and regional analyses in Mongolia over three decades, for more accurate assessment and verification of results, comparison to higher resolution data and field survey must be accompanied.

Acknowledgements

This research was supported by the Asia Research Foundation Grant funded by the Seoul National University Asia Center (#SNUAC-2014-008). I gratefully acknowledge the Remote Sensing Laboratory at Kangwon National University for generously providing NOAA GIMMS NDVI, 30 year local weather station climate data, livestock data, and temperature data.

References

Alcaraz-Segura D, Chuvieco E, Epstein H E, Kasischke E S and Trishchenko A. (2010). Debating the greening vs. browning of the North American boreal forest: differences between satellite datasets Glob. Change Biol. 16 760–70.

Almazroui M. (2011). Calibration of TRMM rainfall climatology over Saudi Arabia during 1998–2009. *Atmos Res* 99: 400–14.

Bai, Y., Wu, J., Xing, Q., Pan, Q., Huang, J., Yang, D., & Han, X. (2008). Primary production and rain use efficiency across a precipitation gradient on the Mongolia Plateau. *Ecology*, *89*(8), 2140–53. Retrieved from http://www.ncbi.nlm.nih.gov/pubmed/18724724

Chapin, F. S. I., Chapin, M. C., Matson, P. A., Vitousek, P. M., & SpringerLink (Online service). (2011). *Principles of terrestrial ecosystem ecology* (2nd ed.). New York: Springer.

de Beurs, K.M., and G.M. Henebry. (2008). Northern Annular Mode effects on the land surface phenologies of Northern Eurasia. Journal of Climate 21: 4257-4279.

Do, N., & Kang, S. (2014). Assessing drought vulnerability using soil moisture-based water use efficiency measurements obtained from multi-sensor satellite data in Northeast Asia dryland regions. *Journal of Arid Environments*, *105*, 22–32. doi:10.1016/j.jaridenv.2014.02.018

Du Plessis, W. P. (1999). Linear regression relationships between NDVI,

vegetation and rainfall in Etosha National Park, Namibia. *Journal of Arid Environments*, *42*(4), 235–260. doi:10.1006/jare.1999.0505

Fang, J., Piao, S., Tang, Z., Peng, C., & Ji, W. (2001). Interannual variability in net primary production and precipitation. *Science (New York, N.Y.)*, *293*(5536), 1723. doi:10.1126/science.293.5536.1723a

Farrar TJ, Nicholson SE, and Lare AR. (1994). The influence of soil type on the relationships between NDVI, Rainfall, and soil moisture in semiarid Botswana. II. NDVI Response to Soil Moisture. *Remote Sens Environ* 50:121-133.

Fensholt R, Rasmussen K, Nielsen TT, and Mbow C. (2009). Evaluation of earth observation based long term vegetation trends — Intercomparing NDVI time series trend analysis consistency of Sahel from AVHRR GIMMS, Terra MODIS and SPOT VGT data. *Remote Sens Environ* 113: 1886–98.

Grist, J., Nicholson, S. E., & Mpolokang, A. (1997). On the use of NDVI for estimating rainfall fields in the Kalahari of Botswana. *Journal of Arid Environments*, *35*(2), 195–214. doi:10.1006/jare.1996.0172

Helldén U and Tottrup C. (2008). Regional desertification: A global synthesis. *Glob Planet Change* 64: 169–76.

Hüttich C, Herold M, Wegmann M, *et al.* (2011). Assessing effects of temporal compositing and varying observation periods for large-area land-cover mapping in semi-arid ecosystems: Implications for global monitoring. *Remote Sens Environ* 115: 2445–59.

Jang, K., Kang, S., Kimball, J. S., & Hong, S. Y. (2014). Retrievals of

All-Weather Daily Air Temperature Using MODIS and AMSR-E Data, 8387–8404. doi:10.3390/rs6098387

Jarvis, A., H.I. Reuter, A. Nelson, E. Guevara, 2008, Hole-filled SRTM for the globe Version 4, available from the CGIAR-CSI SRTM 90m Database (http://srtm.csi.cgiar.org).

Huxman, T. E., Smith, M. D., Fay, P. A., Knapp, A. K., Shaw, M. R., Sala, O. E. (2004). Convergence across biomes to a common rain-use efficiency, (April), 1–4. doi:10.1038/nature02597.1.

Le Houerou, HN. (1984). Rain use efficiency: a unifying concept in arid-land ecology. *J Arid Environ*, 7: 213-247.

Narangarav, D and Lin C. (2011). Investigation of Vegetation Dynamics of Mongolia Using Time Series of NDVI in Response to Temperature and Precipitation. Mongolian Journal of Biological Sciences. 9: 9–17.

Natsagdorj L. and Sarantuya G.(2014). Climate research and observed climate change in Mongolia. 2. Climate Change: observed changes and future projections. Mongolia Second Assessment Report on Climate Change 2014. Ministry of Environment and Green Development of Mongolia.

Lee, H. Y., and Noh, S.C. Advanced Statistical Analysis. (2012). Kwangam Publication.

Nicholson, S. E., & Farrar, T. J. (1994). The Influence of Soil Type on the Relationships between NDVI, Rainfall, and Soil Moisture in Semiarid Botswana . I. NDVI Response to Rainfall, *120*(June), 107–120.

Nicholson SE, Tucker CJ, and Ba MB. (1998). Desertification, drought, and

surface vegetation: An example from the West African Sahel. *Bull of the Am Meteorology Soc* 79: 1-15 815–29.

Noy-Meir, I. (1973). Desert ecosystems: environment and producers. *Annu Rev Ecol And Syst* 4: 25-51.

Paruelo, J. M., Lauenroth, W. K., Burke, I. C., & Sala, O. E. (2014). Grassland Precipitation-Us Across Efficiency Varies a Resource Gradient, *2*(1), 64–68.

Poulter, B., Frank, D., Ciais, P., Myneni, R. B., Andela, N., Bi, J., van der Werf, G. R. (2014). Contribution of semi-arid ecosystems to interannual variability of the global carbon cycle. *Nature*, *509*(7502), 600–603. doi:10.1038/nature13376

Prince SD, Colstoun EB De, and Kravitz LL. (1998). Evidence from rain-use efficiencies does not indicate extensive Sahelian desertification. *Glob Chang Biol* 4: 359–74.

Ricotta, C., Avena, G., & De Palma, A. (1999). Mapping and monitoring net primary productivity with AVHRR NDVI time-series: statistical equivalence of cumulative vegetation indices. *ISPRS Journal of Photogrammetry and Remote Sensing*, *54*(5-6), 325–331. doi:10.1016/S0924-2716(99)00028-3

Rosenzweig, ML. (1968). Net primary production of terrestrial communities: prediction from climatological data. *Am Nat* 102: 67-74.

Sinclair, T. R., Tanner, C. B., & Bennett, J. M. (1984). Water-Use Efficiency Crop Production, BioScience *34*(1), 36–40.

Suttie, J.M., Reynolds S.G., & Batello C (2005). Grasslands of the World. FAO. Rome.

Tarnavsky E, Mulligan M, and Husak G. (2012). Spatial disaggregation and intensity correction of TRMM-based rainfall time series for hydrological applications in dryland catchments. *Hydrol Sci J* 57: 248–64.

Tarnavsky E, Mulligan M, Ouessar M, *et al.* (2013). Dynamic Hydrological Modeling in Drylands with TRMM Based Rainfall. *Remote Sens* 5: 6691–716

Tucker, CJ. (1980). Remote sensing of leaf water content in the near infrared. *Remote Sens Environ* 10:23-32.

Tucker, C. J., Slayback, D. a, Pinzon, J. E., Los, S. O., Myneni, R. B., & Taylor, M. G. (2001). Higher northern latitude normalized difference vegetation index and growing season trends from 1982 to 1999. *International Journal of Biometeorology*, *45*(4), 184–90. Retrieved from http://www.ncbi.nlm.nih.gov/pubmed/11769318

Tucker, C.J., Pinzon, J.E., Brown, M.E., Slayback, D., Pak, E.W., Mahoney, R., Vermote, E. and Saleous, N., (2005). An Extended AVHRR 8-km NDVI Data Set Compatible with MODIS and SPOT Vegetation NDVI Data. International Journal of Remote Sensing, 26(20) 4485-4498.

Tucker, CJ, Pinzon J, Brown M, and GIMMS/GSFC/NASA. (2010). In Hall, Forrest G., G. Collatz, B. Meeson, S. Los, E. Brown de Colstoun, and D. Landis (eds.). ISLSCP II GIMMS Monthly NDVI, 1981-2002. ISLSCP Initiative II Collection. Data set. Available on-line [http://daac.ornl.gov/]

from Oak Ridge National Laboratory Distributed Active Archive Center, Oak Ridge, Tennessee, U.S.A. doi:10.3334/ORNLDAAC/973.

Tsogtbaatar, Jamsran, Khudulmur, S., Dash, D., Batjargal, Z., & Mandakh N. (2014). Desertification Atlas of Mongolia. Institute of Geoecology, Mongolian Academy of Sciences. ISBN: 978-99973-0-197-0.

Turner, N. C. (2004). Agronomic options for improving rainfall-use efficiency of crops in dryland farming systems. *Journal of Experimental Botany*, *55*(407), 2413–25. doi:10.1093/jxb/erh154

UN (United Nations). (1994) UN Earth Summit. Convention on Desertification. UN Conference in Environment and Development, Rio de Janeiro, Brazil, June 3-14, 1992. DPI/SD/1576. United Nations, New York.

Verón, S. R., Paruelo, J. M., & Oesterheld, M. (2006). Assessing desertification. *Journal of Arid Environments*, *66*(4), 751–763. doi:10.1016/j.jaridenv.2006.01.021

Wang N-Y, Liu C, Ferraro R, *et al.* (2009). TRMM 2A12 Land Precipitation Product - Status and Future Plans. *J Meteorol Soc Japan* 87A: 237–53.

Yang, Y., Fang, J., Fay, P. a., Bell, J. E., & Ji, C. (2010). Rain use efficiency across a precipitation gradient on the Tibetan Plateau. *Geophysical Research Letters*, *37*(May), 1–5. doi:10.1029/2010GL043920

Zhongmin, H., Guirui, Y., Jiangwen, F., Huaping, Z., Shaoqiang, W., & Shenggong, L. (2010). Precipitation-use efficiency along a 4500-km grassland transect. *Global Ecology and Biogeography*, *19*(6), 842–851. doi:10.1111/j.1466-8238.2010.00564.x

Appendix 1. Site descriptions for 63 local weather stations.

Natural Zone	Station #	Aimag	Soum	Latitude	Longitude	MAP*	MAT*	Elevation
Desert (n=7)	15	Omnogobi	Gurvantes	43.231	101.043	97.7	5.1	1745
	31	Omnogobi	Bulgan	44.095	103.538	125.0	5.6	1297
	37	Omnogobi	Khanbogd	43.196	107.194	94.4	7.6	1118
	41	Omnogobi	Tsogt-Ovoo	44.423	105.318	100.6	4.4	1294
	66	Khovd	Bulgan	46.095	91.552	82.5	2.9	1214
	68	Dornogobi	Khuvsgul	43.605	109.636	108.8	6.0	1012
	69	Gobi-Altai	Tsogt	44.924	96.754	70.0	5.7	1186
Desert Steppe (n=15)	11	Khovd	Zereg	47.108	92.838	83.1	2.8	1135
	12	Ovorkhangai	Bogd	44.674	102.176	124.5	4.0	1501
	19	Dundgobi	Mandalgovi	45.743	106.264	142.7	2.2	1403
	30	Bayankhongor	Bayankhongor	45.178	101.413	186.5	0.4	1286
	33	Omnogobi	Dalanzadgad	43.577	104.418	120.6	5.2	1458
	45	Bayankhongor	Shinejinst	44.545	99.272	105.0	0.6	2211
	54	Dornogobi	Zamiin-Uud	43.714	111.904	123.7	4.3	972
	59	Zavkhan	Dorvoljin	47.646	94.999	101.4	0.7	1360
	74	Uvs	Zavkhan	48.827	93.112	63.3	1.0	1029
	76	Uvs	Omnogobi	49.105	91.726	140.5	-0.7	1574
	79	Dundgobi	Saikhan-Ovoo	45.461	103.900	115.1	2.5	1318
	94	Khovd	Jargalant	47.996	91.633	134.7	1.0	1398
	97	Dornogobi	Mandakh	44.402	108.250	100.4	4.0	1337
	120	Uvs	Ulaangom	49.972	92.078	157.6	-2.4	933
	125	Dornogobi	Sainshand	44.878	110.119	113.0	4.5	967

Steppe (n=25)	1	Ovorkhangai	Arvaikheer	46.259	102.789	227.2	1.6	1816
	7	Tuv	Ugtaaltsaidam	48.258	105.405	278.4	-0.8	1164
	8	Dornod	Khalkhgol	47.630	118.622	297.1	0.3	686
	18	Selenge	Orkhon	49.144	105.402	296.3	-0.2	751
	39	Uvs	Baruunturuun	49.659	94.404	245.5	-3.2	1218
	43	Khentii	Bayan-Ovoo	47.786	112.111	280.9	0.7	959
	47	Sukhbaatar	Erdenetsagaan	45.909	115.375	273.9	1.8	1070
	49	Tuv	Bayan	47.257	107.538	221.8	-1.3	1405
	52	Tuv	Zuunmod	47.713	106.952	277.5	-0.7	1531
	61	Zavkhan	Tsetsen-Uul	48.748	96.004	245.8	-5.2	1961
	73	Khentii	Ondorkhaan	47.308	110.625	232.5	-0.2	1063
	78	Sukhbaatar	Baruun-Urt	46.673	113.283	204.4	1.4	982
	81	Arkhangai	Erdenemandal	48.529	101.368	273.4	0.0	1515
	84	Khuvsgul	Renchinlkhumbe	51.109	99.669	287.1	-6.8	1592
	85	Dornod	Matad	46.955	115.296	231.1	1.7	911
	87	Bayan-Olgii	Bulgan	46.930	91.082	133.0	-1.5	1958
	89	Zavkhan	Bayantes	49.700	96.364	190.0	-0.2	1407
	93	Sukhbaatar	Bayandelger	45.730	112.355	167.6	2.2	1118
	96	Tuv	Erdenesant	47.333	104.493	249.7	1.1	1340
	101	Gobi-Altai	Tonkhil	46.304	93.911	111.0	-0.2	2193
	102	Bayankhongor	Bayanbulag	46.812	98.087	135.7	-3.7	2262
	128	Dornod	Dashbalbar	49.551	114.404	283.6	0.5	710
	21	Bayan-Olgii	Altai	48.299	89.515	131.5	-2.8	2235
	50	Bayan-Olgii	Olgii	48.980	89.938	127.9	1.1	1721
	64	Bayankhongor	Galuut	46.702	100.143	197.8	-4.2	2122

Forest Steppe (n=16)	2	Orkhon	Bayan-Ondor	49.037	104.086	362.4	0.9	1335
	29	Selenge	Sukhbaatar	50.243	106.173	286.6	0.8	607
	35	Khuvsgul	Murun	49.639	100.167	240.1	-0.2	1274
	36	Selenge	Eroo	49.749	106.661	274.6	-1.4	680
	38	Ulaanbaatar	Ulaanbaatar	47.919	106.848	273.1	-1.5	1353
	46	Bulgan	Khutag-Ondor	49.394	102.710	296.5	-0.5	949
	57	Ovorkhangai	Khujirt	46.900	102.772	283.3	-1.0	1639
	72	Arkhangai	Erdenebulgan	47.471	101.463	337.1	1.0	1668
	75	Zavkhan	Tosoltsengel	48.760	98.262	238.7	-5.6	1720
	105	Khentii	Dadal	49.022	111.612	401.6	0.2	1032
	114	Zavkhan	Uliastai	47.727	96.848	215.8	-1.6	1750
	122	Selenge	Bayangol	48.913	106.090	289.9	-0.1	822
	124	Arkhangai	Tariat	48.157	99.877	235.7	-3.3	2050
	126	Khuvsgul	Tarialan	49.609	101.985	300.5	0.0	1214
	127	Khuvsgul	Khatgal	48.951	99.534	302.3	-4.1	1709
	129	Bulgan	Bulgan	48.818	103.519	335.3	-0.1	1221

*MAP: Mean Annual Precipitation; MAT: Mean Annual Temperature

국문초록

몽골지역의 30년 기후자료 분석에 의한 가뭄 취약성 연구

이 지 선

서울대학교 환경대학원

환경계획학과 환경관리전공

2015년 2월

지도교수 이 도 원

건조지(drylands)는 기후적 요인과 인간의 활동으로 인한 사막화와 토지 황폐화에 특히 취약하기 때문에 건조 및 반건조 생태계에 대한 연구는 기후 변화에 대응과 적응에 관련하여 의미가 있다. 500 mm 미만의 낮은 연강수량을 보이는 지역에서는 많은 경우 강수량이 식생 생산성의 제한 요인이다. 기존의 연구들은 대규모의 토지 황폐화와 기후 변화에 대한 생태계의 반응을 평가하기 위해서 순일차 생산성과 연간 강수량을 바탕으로 한 강수이용효율지수(Rain Use Efficiency; RUE)를 사용했다. 본 연구에서는 몽골에서의 가뭄 스트레스와 가뭄 취약성(민감성)을 평가하기 위해 Do and Kang(2014)의 토양수분효율지수를 바탕으로 한 가뭄 스트레스 지수와 가뭄 취약성 지수를 계산법을 RUE로 변환시켜 적용하였다.

이 연구의 목적은 먼저, 몽골에서 1982년에서 2008년까지(27년 간)의 강수이용효율지수 와 가뭄 취약성의 시간적 변화를 분석하는 것이다. 이는 첨단 고해상 방사계 위성 자료(Advanced Very High Resolution Radiometer)를 사용해서 성장기인 6월에서 9월에 측정된 정규식생지수와 63개의 지역 기상 관측소의 강수량 자료를 사용했다. 두 번째로, 강수이용효율지수 와 가뭄 취약성의 공간적 분포를 분석 하였다. 이는 1998년에서 2008년, 즉 11년에 동안의 픽셀 자료인 정규식생지수 지도와 열대 강우 관측 위성(Tropical Rainfall Measuring Mission)의 강수량 자료를 바탕으로 했다. 마지막으로, 약 300개의 쏨 단위의 회귀 분석을 통해 기후, 지리, 토지 이용 요소들이 가뭄 스트레스에 미치는 영향을 분석했다.

63개 지역 기상관측소를 4개의 초지(steppe) 지역으로 구분하여 분산분석을 시행했다. 사막 지역이 가장 높은 가뭄 스트레스와 가뭄 취약성을 보였고, 초지 지역은 가장 낮은 가뭄 스트레스를, 그리고 삼림 초지가 가장 낮은 가뭄 취약성을 보였다. 특히 바얀콩고르(Bayankhongor) 아이막 남부 지방인 바얀 온도르(Bayan Ondor) 쏨과 시네신스트(Shinejinst) 쏨, 그리고 고비 알타이(Gobi-Altai) 아이막의 에르덴(Erdene) 쏨의 남쪽 지역이 픽셀 지도를 통해 볼 때 높은 가뭄 스트레스를 보였다. 각각 쏨의 평균 값을 이용한 회귀분석의 결과로는 높은 인구밀도, 온도, 그리고 강수이용효율지수가 높은 가뭄 스트레스로 이어지고, 높은 목축밀도와 강수량은 가뭄 스트레스를 낮추는 것으로 나타났다. 그리고 가뭄 스트레스는 사막과 비교해 볼 때 스텝 지역과 사막 스텝에

서 보다 낮았다.

강수이용효율지수의 사용은 몽골의 초목생산성 예측, 토지 황폐화 평가와 가뭄반응예측을 가능하게 하였다. 몽골지역의 30여년의 인공위성 자료는 장기간의 분석과 넓은 범위의 공간 분석에는 유용하지만 좀 더 정확한 평가 및 결과에 대한 확증을 위해서는 고해상도 데이터의 비교와 현지조사가 필요할 것이다. 건조지 생산성과 가뭄 취약성에 대한 평가는 강수량 변화와 온도 상승과 같은 기후변화에 대응하기 위한 미래 토지관리 계획에 유용할 것이다.

주요어 : 가뭄 취약성, 강수이용효율지수(Rain Use Efficiency), 몽골, AVHRR NDVI, 기후변화

학 번 : 2012 - 23806